Journal of the European Ceramic Society **19** (1999) 2133–2144

PII: S0955-2219(99)00022-9
0955-2219/99/$ - see front matter

Effect of Different Fiber Orientations on Compressive Creep Behavior of SiC Fiber-reinforced Mullite Matrix Composites

Zhen-Yan Deng[a,b,c,1]

[a]Korea Institute for Advanced Study, 207-43 Cheongryangri-dong, Dongdaemun-gu, Seoul 130-012, Republic of Korea
[b]Superplastic Nanoscience Laboratory, National Industrial Research Institute of Nagoya Hirate-cho, Kita-ku, Nagoya 462-8510, Japan
[c]The State Key Laboratory of High Performance Ceramics and Superfine Microstructure, Shanghai Institute of Ceramics, Chinese Academy of Sciences, Shanghai 200050, People's Republic of China

(Received 17 September 1998; accepted 23 January 1999)

Abstract

The compressive creep behavior of monolithic mullite and a composite made of mullite reinforced by 40 vol% SiC fiber were investigated at temperatures from 1100 to 1200°C and under stresses from 5 to 55 MPa in air with a loading direction parallel and perpendicular to the fiber direction. For both situations the composite exhibits better creep resistance than monolithic mullite, although there is a creep anisotropy. The improvement in creep resistance when the fibers are parallel to the loading directions is due to the shedding of the applied stress on the SiC fibers, and the improvement in creep resistance when the fibers are perpendicular to the loading direction occurs because the fibers inhibit the lateral deformation of the mullite matrix along the fibers. The improvement mechanisms of the composites were confirmed further by their creep-recovery study, which indicated that the two types of composite specimens exhibit both an apparent creep-recovery behavior on load removal, due to the relaxation of the residual stress state between the mullite matrix and the SiC fibers after unloading. © *1999 Elsevier Science Limited. All rights reserved*

Keywords: composites, creep, mechanical properties, SiC fiber, mullite.

1 Introduction

SiC fiber-reinforced ceramic matrix composites have received considerable attention in the past few years, due to their potential application in the aeronautics and space industry. The fracture toughness and strength of composites are strongly influenced by the interface bonding between the fibers and matrix.[1–4] It is found that a suitable fiber/matrix bonding is favorable for the enhancement in the mechanical property of composites. The investigations on the high-temperature creep behavior of composites are not known as well as the room-temperature mechanical properties, due to the cost of the equipment for creep tests and the difficulties in correctly conducting creep tests. However, before the composites can be used in practical structural applications at elevated temperatures, a greater understanding of their creep characteristics and mechanisms must be known. Previously, several groups have devoted their efforts to the investigations on the creep behavior of fiber-reinforced ceramic matrix composites.[5–16] Chermant *et al.*[5–9] studied the flexural and tensile creep behavior of 1D, 2D SiC- and 2·5D C-fiber reinforced ceramic matrix composites, and found a threshold stress for the creep, which corresponds to the stress for matrix cracking. Damage creep is responsible for the strain with mainly damage accumulation in the transient creep stage, and damage mechanisms involve opening and coalescence of the preexisting cracks, matrix microcracking and delamination. Evans and Weber[10] studied the tensile creep behavior of a 0°/90° SiC_f–SiC composite with a plain weave, and found that the creep rate of the composite above a threshold is dominated by the creep viscosity of the fibers. They concluded that the creep performance of CMCs must be addressed by improving the creep resistance of the fibers, and increasing the creep resistance of the matrix does not have an appreciable

[1]Correspondence address, see affiliation a.
E-mail: zydeng@kias.re.kr.

effect. Zhu *et al.*[11,12] studied the effect of the additives in the matrix on the creep and environmental resistance of the 0°/90° SiC_f–SiC composite, and found that the creep and fatigue properties for the composite in air at high temperatures was improved, due to the fact that the filling of the glassy phases in the cracks prohibited the diffusion of oxygen from the environment. Holmes *et al.*[13,14] studied the tensile creep behavior of SiC fiber-reinforced Si_3N_4 matrix and calcium aluminosilicate matrix composites and found that, in addition to the intrinsic creep property of the constituents, the transient redistribution in stress between the fibers and matrix plays a key role in the overall creep behavior and the microstructural damage modes that occur during creeping. Weber *et al.*[15] and Thayer *et al.*[16] studied the creep anisotropy of SiC fiber-reinforced ceramic matrix composites, and their results indicated that different loading states (in tension, bending and compression) on the composite specimens would cause different creep stress exponents. Because the structural components might sustain varieties of stress states in the working environments, the study of the creep anisotropy of composites is necessary. In this paper, the effect of different fiber orientations on the compressive creep behavior of SiC fiber-reinforced mullite matrix composites will be studied.

2 Experimental Procedure

In this investigation, Nicalon-SiC fibers with the diameter of 10–25 μm (Type NLM 102-SiC fiber, Nippon Carbon Co. Ltd., Japan) were used as the reinforcement agent in mullite matrix. The mullite matrix was made from a commercially available mullite powder with a mean grain size of about 1 μm. The 1D composite was fabricated by incorporating the mullite around each fibers according to a specific process. Because of the poor sinterability of mullite[17,18] and the change in the Nicalon-SiC fibers, at over 1300°C[19], about 4·6 vol% of the Li_2O-Al_2O_3-SiO_2 (LAS) glass powder (Li_2O: 3 wt%; SiO_2: 23 wt% and $A1_2O_3$: the balance; particle $< 2\,\mu$m) was added in the mullite matrix. This sintering aid is added during the ball milling in ethanol for 24 h for reducing the sintering temperature of the monolith and composite. The final consolidation of the matrix monolith and the composite was done by hot-pressing at 25 MPa and 1250°C for 45 min in a nitrogen atmosphere with a cooling rate not lower than 400°C h^{-1}. These steps produced a fully densified monolithic mullite (presently mullite + LAS glass phase) and composite (mullite + LAS glass phase + SiC fibers) with a porosity less than 1%. The glass phase both in monolithic mullite and in composites do not crystallize during hot-pressing and the following cooling process as the glass can only become glass-ceramics by holding at around 700–800°C for several hours. The composite which contained 40 vol% Nicalon-SiC fibers was used in the following investigation.

The hot-pressed monolithic mullite and composite plates were ground and cut to $4 \times 4 \times 6\,mm^3$ rectangular specimens for compressive creep tests. Two types of composite specimens were used in the experiments: one with the fiber direction parallel to the applied stress, referred as [0°] composite; the other with the fiber direction perpendicular to the applied stress, referred as [90°] composite (Fig. 1). The compressive creep equipment and data acquisition system used in our study are similar to those used by Weber *et al.*[15] The compressive creep strain was calculated by the relative displacement between the top and bottom surfaces of the creep specimens, which was measured by an extensometer with an accuracy of $\pm 1\,\mu$m. The compressive creep tests were conducted in air atmosphere at 1100°C–1200°C and under the nominal constant stress of 5–55 MPa, with the temperature controlled to within ± 2°C during each test. At the same time, the specimens were held at testing temperature for at least 30 min before applying the load. The number of the creep specimens for monolithic mullite or each type of composite was at least six, in order to study the variations in creep strain rate with stress and temperature.

The creep-recovery behavior for two types of composites was investigated by applying the load for a given period of time, almost totally removing the load for an additional time, and then reloading to the original level during creep tests.[13,14] This procedure was repeated more than four times to obtain information on the dependence of the anelastic recovery on the total creep strain. A small residual load (~2 MPa) was left on each specimen

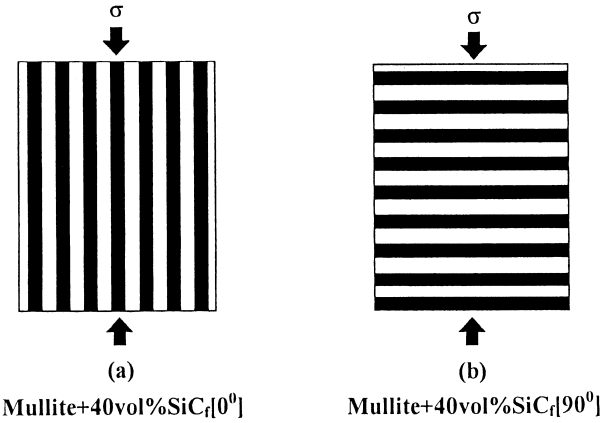

Fig. 1. Schematic representation of the two types of composite specimens: (a) [0°] composite with the fiber direction parallel to the load direction and (b) [90°] composite with the fiber direction perpendicular to the load direction.

in the 'unload' condition to maintain the integrity of the loading assembly and to facilitate easy and rapid reloading. In order to test the reliability of experimental results, at least two specimens for each type of composite were used for creep-recovery behavior tests.

The as-received and crept specimens were cleaved using a knife in the direction of the fibers and analyzed by scanning electron microscopy (SEM). The creep experimental data were processed via a personal computer.

3 Results

3.1 Material characterization

In order to understand the distribution of fibers in mullite matrix, cross-sections of [0°] composite were prepared by grinding and polishing up to the 1 μm diamond grade, and were observed by optical microscope (Fig. 2). From this figure, it can be seen that there is a spread size distribution for SiC fibers, and in general the SiC fibers are distributed uniformly in mullite matrix. Figure 3 shows a fracture surface of the as-received composite specimen obtained after cleavage along the fiber direction. In Fig. 3, it can be clearly seen that the fibers easily pull-out from the matrix. The surfaces of fibers are smooth, indicating a relative weak bonding between the SiC fibers and mullite matrix, which is favorable for the improvement in the fracture toughness of composites.[1,20] No apparent change in the size and morphology of matrix mullite grains was observed after hot-pressing, due to the thermal stability of mullite at the hot-pressing temperature.[17,18,21] That was confirmed by the SEM observation on the thermal etching surfaces of monolithic mullite specimens.[22] Ohira *et al.*[21] studied the relationship between the microstructures of single-phase mullite and the sintering temperature, and found that the size of mullite grains starts to increase at about 1600°C and the equiaxed grain morphology of mullite becomes elongated over 1650°C. The hot-pressing temperature at 1250°C adopted in our experiments is much lower than the temperature which causes the change in the grain size and morphology of mullite, and the matrix grains in monolithic mullite and composite would change little during the hot-pressing process.

3.2 Creep behavior

In the creep experiments, all monolithic mullite and composite specimens were crept to reach a roughly minimum strain rate. We found that all monolithic mullite and composite specimens showed three creep stages. Figure 4 shows the typical creep curves for monolithic mullite and two composite specimens. We can see that the creep resistance of the composite specimens is apparently higher than that of monolithic mullite, and the rank of the creep resistance is [0°] composite > [90°] composite > monolithic mullite, indicating a creep anisotropy due to the fiber orientation in the composites. In Fig. 4, only the creep curve for monolithic mullite at 1100°C is presented. If the creep curve of monolithic mullite at 1200°C was plotted it would be steeper than that at 1100°C, because the creep resistance of ceramic materials decreases with the increase in creep temperature.[23]

The stress and temperature dependence of steady-state or minimum creep rates for the three materials are shown in Figs 5 and 6, respectively. The results shown in Figs 5 and 6 also indicate that, in spite of the creep anisotropy for the different fiber orientations in the composites, the addition of SiC fibers in monolithic mullite enhances considerably the creep resistance of mullite materi-

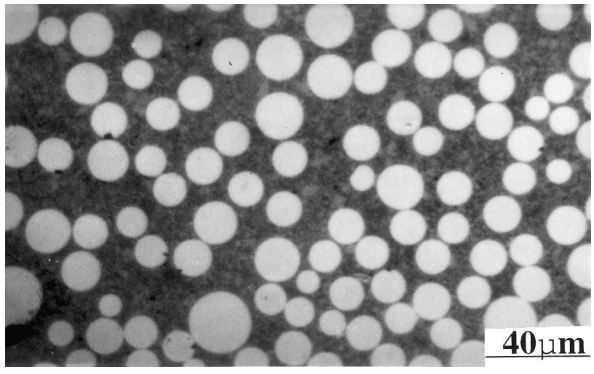

Fig. 2. Optical micrograph of a cross-section of a composite specimen.

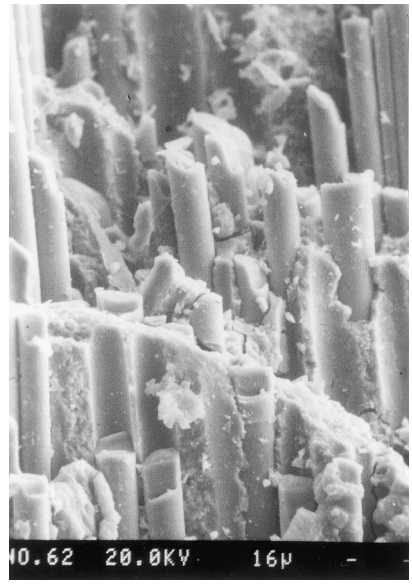

Fig. 3. SEM micrograph of a fracture surface of the as-received composite specimen.

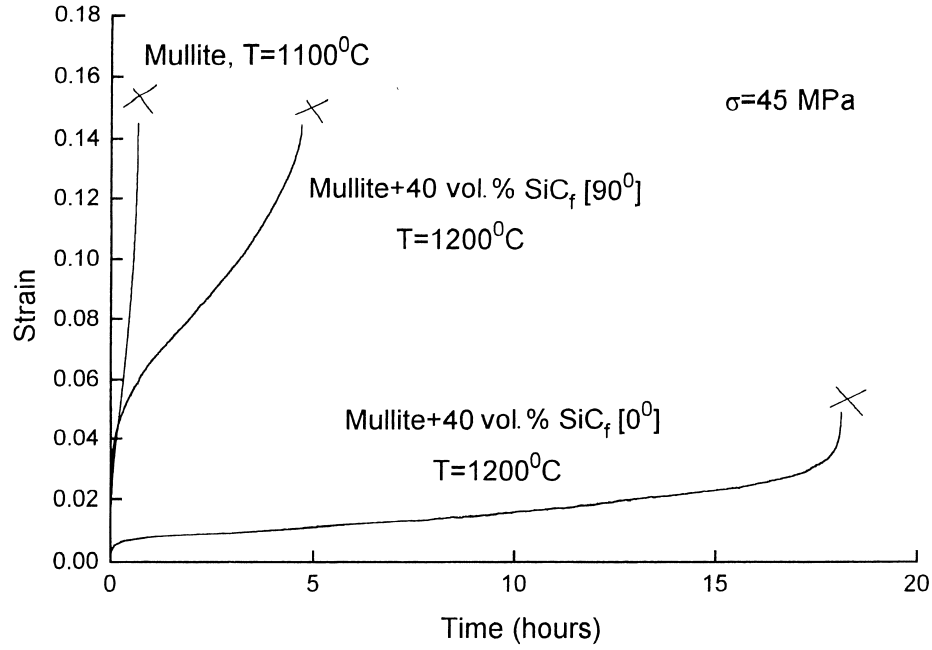

Fig. 4. Compressive creep curves of monolithic mullite and the two types of composite specimens under 45 MPa, where all of the monolithic mullite and composite specimens fractured in the creep tests.

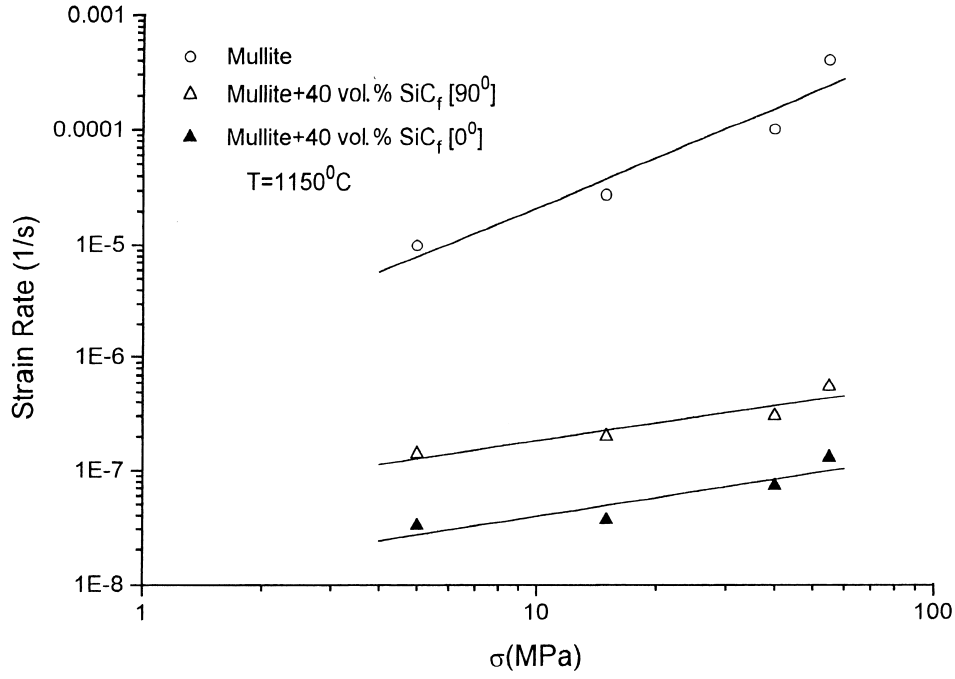

Fig. 5. Stress dependence of the steady-state creep rate for monolithic mullite and the two types of composite specimens at $T = 1150°C$.

als. Roughly, the strain rate of [0°] composite is about three orders of magnitude lower than that of monolithic mullite, but the strain rate of [90°] composite is only about 4–6 times higher than that for the [0°] composite. The difference in strain rate between [90°] composite and [0°] composite decreases with the decrease in temperature. These results are very different from the implication of Weber *et al.*,[15] that the fibers with orientation perpendicular to the applied stress could not improve the creep resistance of composites. Wu *et al.*[14] studied the tensile creep behavior of a 2D SiC_f–CAS composite, and found that the [90°] fibers in the composites restrict the movement of the [0°] fibers by their direct contact, but how much of the effect of the [90°] fibers on the creep resistance of the composites in tension and compression is unclear.

The creep stress exponents and creep activation energies for the three materials were obtained by apparent linear fitting of the data in Figs 5 and 6 (Table 1). Table 1 indicates that, the stress exponent 1·42 of monolithic mullite approaches the

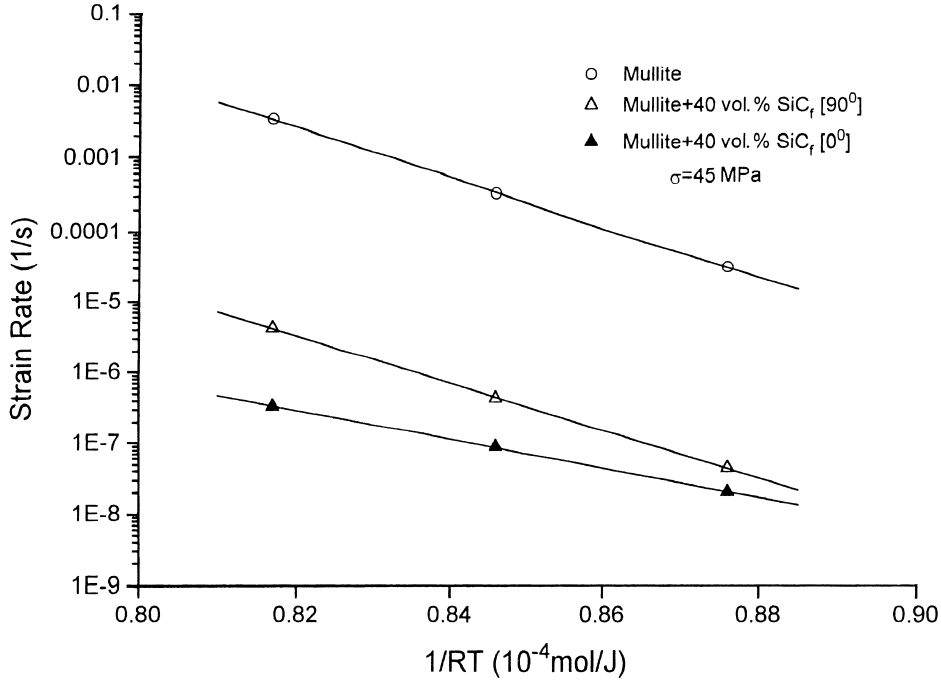

Fig. 6. Arrhenius plots for monolithic mullite and the two types of composites under $\sigma = 45$ MPa.

Table 1. The value of the creep stress exponent, n, at $T = 1150°C$ and the creep activation energy, ΔQ, under $\sigma =$ 45 MPa for monolithic mullite and the two types of composites

Materials	n	$\Delta Q(kJ\ mol^{-1})$
Mullite	1·42	791
Mullite + 40 vol% SiC_f [0°]	0·55	472
Mullite + 40 vol% SiC_f [90°]	0.52	769

value of 1·6 of the mullite contained a small amount of glass phase obtained by Hynes *et al.*,[24] and is different from that of the two composites. The stress exponent 0·55 for the [0°] composite is close to the value 0·52 obtained for the [90°] composite. But these values are smaller than those for SiC_f–CAS composites[14,15] obtained by creep tests in tension, bending and compression. The lower stress exponent for our composites may be partly due to the lower stress range used in our creep experiments. The activation energy of 791 kJ mol^{-1} for monolithic mullite also approaches the value of 742 kJ mol^{-1} for the mullite contained a small amount of glassy phase.[24] At the same time, the activation energy 472 kJ mol^{-1} for the [0°] composite is much smaller than that for the monolithic mullite, but the activation energy 769 kJ mol^{-1} for the [90°] composite is close to that for the monolithic mullite.

3.3 Creep-recovery behavior

The creep-recovery behavior for the two composites is shown in Figs 7 and 8. It indicates that there is an apparent anelastic recovery on load removal for the two composites. The definitions of total-strain recovery ratio R_t and creep-strain recovery ratio R_{cr} in Figs 7 and 8 are the same as those given by Holmes *et al.*,[13,14] where R_t, is defined as the sum of the elastic and creep strains recovered in a particular cycle divided by the total accumulated strain that exists before the unloading, and R_{cr} is defined as the creep strain recovered during a particular unloading cycle divided by the creep strain for the cycle. In fact, the creep-recovery behavior obtained by compressive creep tests for our composites is analogous to that proposed by Holmes *et al.*[13] obtained by tensile creep tests for the SiC fiber-reinforced Si_3N_4 matrix composites, the creep-strain recovery ratio R_{cr} increases and the total-strain recovery ratio R_t decreases with the increase in the creep cycle. In addition, the monolithic mullite should have no anelastic recovery on load removal during creep tests, because the grain morphology of monolithic mullite is equiaxed and the creep-recovery behavior is produced mainly by the residual stress between the different microstructure phases of ceramic materials after removing the load.[13,14,25]

4 Discussion

4.1 Creep mechanisms and oxidation reactions

High purity mullite is considered as a prime candidate material for high temperature structural applications, due to its excellent thermal stability at elevated temperature. It exhibits excellent creep resistance up to 1500°C, and the diffusional creep mechanism is its principal creep mechanism.[21,26,27]

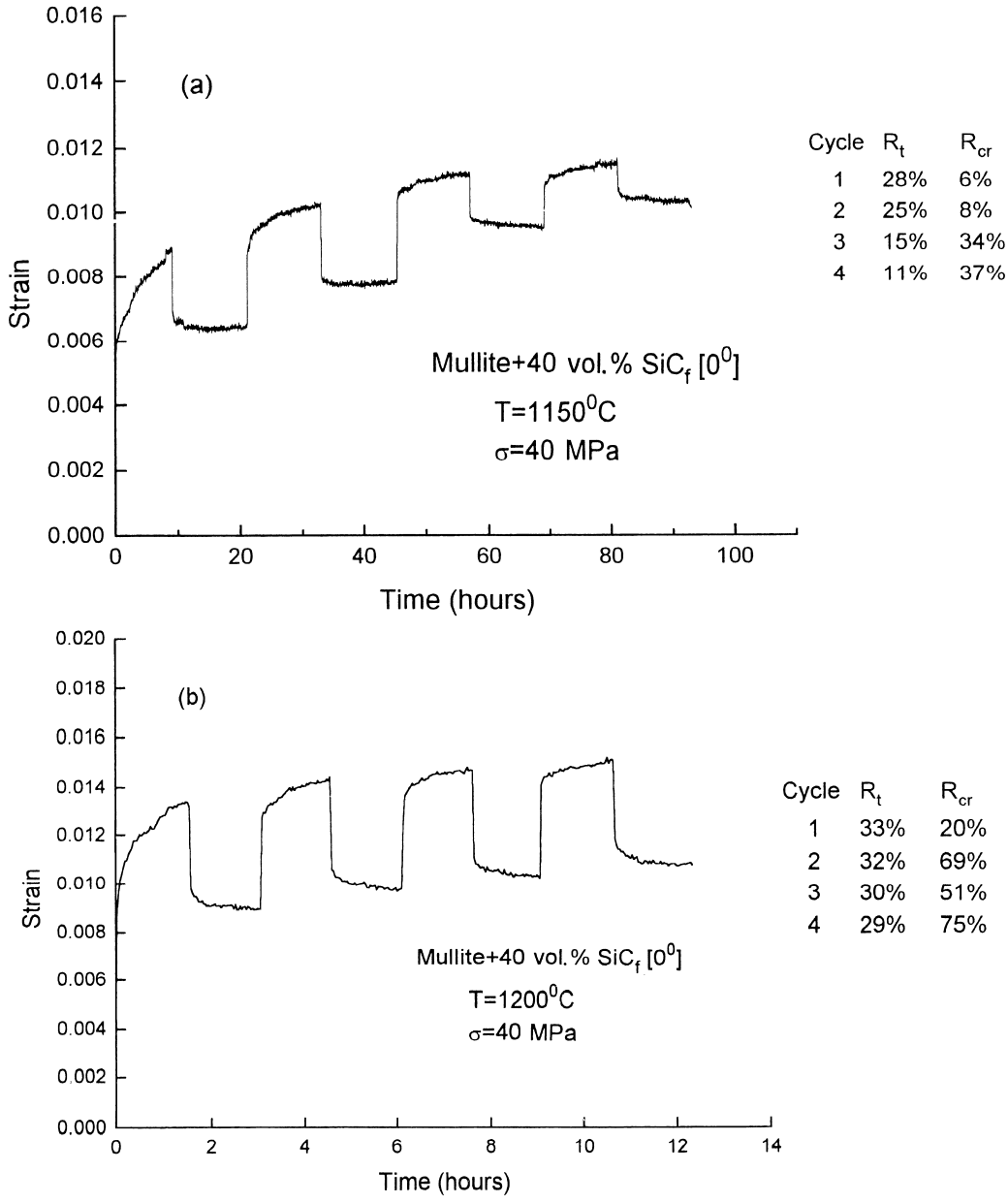

Fig. 7. Strain versus time for the [0°] composite specimens showing the effect of the load removal tested (a) at 1150°C under 40 MPa and (b) at 1200°C under 40 MPa, where the sustained time of loading and unloading is the same.

The monolithic mullite and mullite matrix of the composites in this study contained a small amount of a glassy phase, and they have poor creep resistance[24] compared to the SiC fibers. Meanwhile, a greater difference in creep resistance between mullite matrix and SiC fibers is favorable for the anisotropy analyses of the composites with the different fiber orientations. Hynes *et al.*[24] studied the creep behavior of a mullite containing about 3∼8 wt% glass phase, and found that the creep mechanism of mullite is a viscous flow mechanism. Because the glassy phase in our mullite matrix softens at over 1000°C,[28] the creep of monolithic mullite and of the composites is also governed by a viscous flow mechanism. The viscous glassy phase in the mullite matrix would flow onto the side surfaces of the specimens during creep tests, due to the compressive stress, and these viscous glassy phases could be devitrified during the cooling process after the end of creep test (Fig. 9). The stress exponent and activation energy of monolithic mullite close to those of Hynes *et al.*[24] also verifies this deduction. The size and morphology of matrix mullite grains might have no apparent changes, as the temperatures for creep tests are below 1250°C, as proposed from the observations of Ohira *et al.*[27] on the crept specimens of mullite ceramics. The results of Ohira *et al.*[27] indicated that, the mullite grains grow slightly from the average size of 1·2 to 1·6 μm after a creep test at 1500°C during the long term in the case of mullite, but the elongation of mullite grains is not clearly observed.

Figures 10 and 11 show the fracture surface features of the composite specimens being crept at

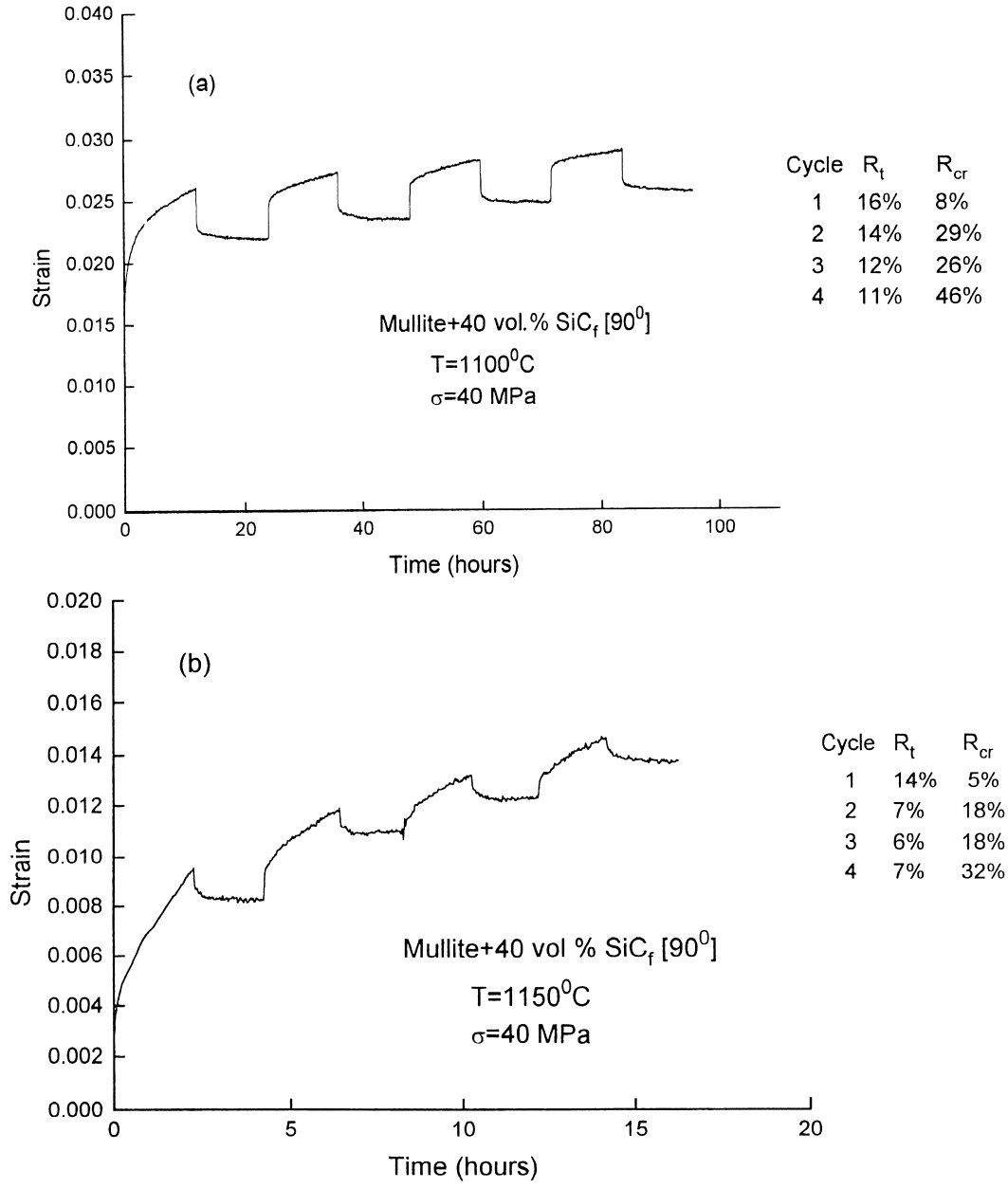

Fig. 8. Strain versus time for the [90°] composite specimens showing the effect of the load removal tested (a) at 1100°C under 40 MPa and (b) at 1150°C under 40 MPa, where the sustained time of loading and unloading is the same.

different temperatures, after cleavage. In Fig. 10, it can be seen that the fibers are pulled out from the mullite matrix easily and the surfaces of the fibers in crept composite specimens are as clean as those in the as-received composite specimen, indicating no apparent oxidation reactions on the surfaces of the SiC fibers at 1100°C. The situation of the crept composite specimen at 1150°C is different: the fibers can not be pulled-out from the mullite matrix and there are some apparent oxidation reactions on the surfaces of the SiC fibers (Fig. 11). The oxidation reactions on the surfaces of SiC fibers, at over 1150°C would decrease the strength of the fibers[29] and increase the interface bonding between the fibers and mullite matrix.

4.2 Model analyses

According to the fiber orientation regarding the loading direction, the creep behavior of the composites could be deduced from the creep resistance of the SiC fibers and mullite matrix from the rule of mixtures.[30]

4.2.1 [0°] composite

For the [0°] composite, the total strain rate of each constituent, $\dot{\varepsilon}_{i,\mathrm{tot}}$ is given by the sum of the elastic strain rate, $\dot{\varepsilon}_{i,\mathrm{el}}$, and the inelastic creep strain rate, $\dot{\varepsilon}_i$. To satisfy compatibility, this sum must be equal to the total strain rate of the composite, $\dot{\varepsilon}_{c,\mathrm{tot}}$:

$$\dot{\varepsilon}_{c,\mathrm{tot}} = \dot{\varepsilon}_{i,\mathrm{tot}} = \dot{\varepsilon}_{i,\mathrm{el}} + \dot{\varepsilon}_i = \dot{\sigma}_i/E_i + \dot{\varepsilon}_i \qquad (1a)$$

or:

$$\dot{\sigma}_i = E_i(\dot{\varepsilon}_{c,\mathrm{tot}} - \dot{\varepsilon}_i) \quad (i = \text{ fiber, matrix}) \tag{1b}$$

where E_i is the Young's modulus of the constituent and σ_i the stress supported by the constituent in the composite. The stress on each constituent can be expressed in terms of the volume fraction of the constituent:

$$\sum_{i=\text{ fiber, matrix}} V_V(i)\sigma_i = \sigma_c \tag{2a}$$

or:

$$\sum_{i=\text{ fiber, matrix}} V_V(i)\dot{\sigma}_i = \dot{\sigma}_c \tag{2b}$$

where $V_V(i)$ is the volume fraction of the constituent and σ_c the stress applied on the composite. From eqns (1b) and (2b), one obtains the total strain rate of the composite:

$$\dot{\varepsilon}_{c,\mathrm{tot}} = \frac{1}{E_c''}(\dot{\sigma}_c + \sum_{i=\text{ fiber, matrix}} V_V(i)E_i\dot{\varepsilon}_i) \tag{3}$$

where:

$$E_c'' = \sum_{i=\text{ fiber, matrix}} V_V(i)E_i \tag{4}$$

is the axial modulus of the composite. The first and second parts of the right side of eqn (3) represent the elastic component and inelastic creep component of the composite strain rate, respectively. As the loading process is finished, the stress applied on the composite specimen is invariant with time, and $\dot{\sigma}_c = 0$. From eqn (3), one can conclude that, the overall creep rate of [0°] composite is equal to the weighted mean value of the constituent inelastic creep rates, $\dot{\varepsilon}_i$, with a weighted factor $V_v(i)E_i/E_c$. During the primary creep stage, a stress redistribution between the fibers and matrix occurs, due to the mismatch in the elastic and inelastic creep properties between the fibers and matrix. When the composite creeps to reach the stable-state creep stage, the stress redistribution between the fibers and the matrix stops, and the elastic strain rates of the fibers and the matrix in eqn (1) should be zero: $\dot{\varepsilon}_{i,\mathrm{el}} = 0$. In this creep stage, the creep strain rate of the fibers and the matrix should be the same, and is equal to the creep strain rate of the composite. This implies that the SiC fibers in [0°] composite would support most part of the applied stress[23] when the fiber volume fraction is of the same order of magnitude than that of the mullite matrix, because the creep resistance of the SiC fibers is much higher than that of the mullite matrix in our composites. Therefore, *the creep properties of [0°] composite should be determined by the creep property of the SiC fibers*.

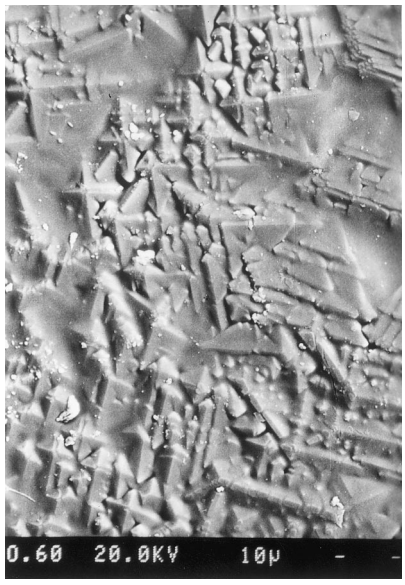

Fig. 9. SEM micrograph of the devitrification on the side surface of [0°] composite specimen being crept for 97 h at $T = 1150$°C under 40 MPa.

4.2.2 [90°] Composite

For [90°] composite, the stress on each constituent is the same and is equal to the stress applied on the composite. The composite strain is the sum of the strains of all constituents:

$$\begin{aligned}\varepsilon_{c,\mathrm{tot}} &= \sum_{i=\text{ fiber, matrix}} V_V(i)\varepsilon_{i,\mathrm{tot}} \\ &= \sum_{i=\text{ fiber, matrix}} V_V(i)(\varepsilon_{i,\mathrm{el}} + \varepsilon_i) \\ &= \sum_{i=\text{ fiber, matrix}} V_V(i)(\sigma_i/E_i + \varepsilon_i) \\ &= \sigma_c/E_c^{\perp} + \sum_{i=\text{ fiber, matrix}} V_V(i)\varepsilon_i\end{aligned} \tag{5}$$

where:

$$E_c^{\perp} = 1/\left(\sum_{i=\text{ fiber, matrix}} V_V(i)/E_i\right) \tag{6}$$

is the modulus of the composite in the direction perpendicular to the fibers. The strain rate of composite can be obtained from eqn (5):

$$\dot{\varepsilon}_{c,\mathrm{tot}} = \dot{\sigma}_c/E_c^{\perp} + \sum_{i=\text{ fiber, matrix}} V_V(i)\dot{\varepsilon}_i \tag{7}$$

The first and second parts of the right side of eqn (7) represent the elastic component and inelastic creep component of the composite strain rate, respectively. As the loading process is finished, the stress applied on the composite specimen is constant, and $\dot{\sigma}_c = 0$. From eqn (7), we can conclude

that, the overall creep rate of [90°] composite is equal to the weighted mean value of the constituent creep rates, $\dot{\varepsilon}_i$, with a weighted factor $V_V(i)$. As the creep resistance of SiC fibers is much higher than that of the mullite matrix, the creep strain rate of the mullite matrix is much faster than that of the SiC fibers, due to the same stress applied on the matrix and fibers in the [90°] composite. Therefore, *the creep properties of the [90°] composite should be governed by the creep property of the mullite matrix* if the volume of mullite matrix is larger than that of the SiC fibers, which is consistent with the implication of Weber *et al.*[15]

4.3 Improvement mechanisms of composite creep resistance

The results of our creep experiments showed that, the strain rate of the [0°] composite is about three orders of magnitude lower than that of monolithic mullite, indicating the creep behavior of the [0°] composite is governed by the creep behavior of the SiC fibers, which is in good agreement with the model analyses above. The stress exponent and activation energy of [0°] composite approach those of the Nicalon SiC fibers in tensile creep tests,[31] where a stress exponent 0·97 at 1100°C and an activation energy 300∼500 kJ mol^{-1} for the Nicalon SiC fibers were obtained, also confirms that the creep behavior of the [0°] composite is controlled by the SiC fibers.

However, the experimental results for the [90°] composite are not consistent with those given by model. Because the [90°] composite also exhibited excellent creep resistance compared with the creep behavior of monolithic mullite, the strain rate of [90°] composite is about 4–6 times higher than that of the [0°] composite. The difference between the model and the experimental results may be due to that the fact that the model does not consider the interactions between the SiC fibers and mullite matrix during creep for the [90°] composite. In fact, the SiC fibers in the [90°] composite would inhibit the sliding of mullite matrix grains along the fiber direction during creep tests, due to the friction between the SiC fibers and mullite matrix under the compressive stress. The stress exponent of the [90°] composite is almost the same as that of the [0°] composite confirms the contribution of the SiC fibers to the creep resistance of the [90°] composite. As the SiC fibers in the [90°] composite enhance considerably the creep resistance of mullite materials, and the creep property of the [90°] composite is also governed by the creep property of the SiC fibers. In addition, the activation energy of the [90°] composite is close to that of monolithic mullite. It may reflect the dependence of the viscosity of boundary glassy phase on the temperature.[24,8] Fig. 11 showed that the oxidation reactions on the surfaces of SiC fibers at over 1150°C increase the interface bonding between the fibers and mullite matrix, and the strengthened interface bonding may be favorable for inhibiting matrix grain motion along the fiber surfaces in the [90°] composite.

The improvement mechanisms of the creep resistance for two types of composites can be also seen from their creep-recovery behavior, because there is an apparent creep-strain recovery after unloading. Figures 12 and 13 show the stress redistribution between the SiC fibers and mullite matrix in the [0°] and [90°] composites for the stress parallel to the fiber direction during compressive creep and creep recovery. As the creep resistance of

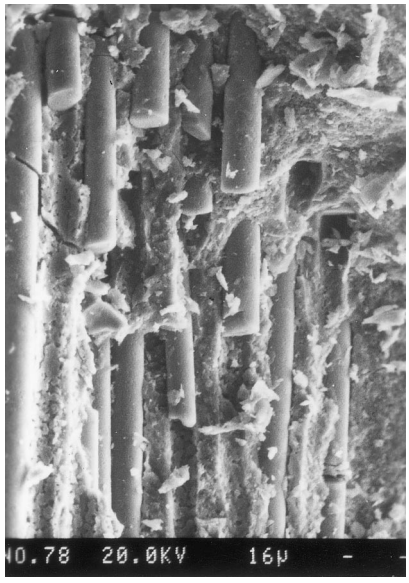

Fig. 10. SEM micrograph of the fracture surface of the [0°] composite specimen being crept for 36 h at $T = 1100$°C under 40 MPa.

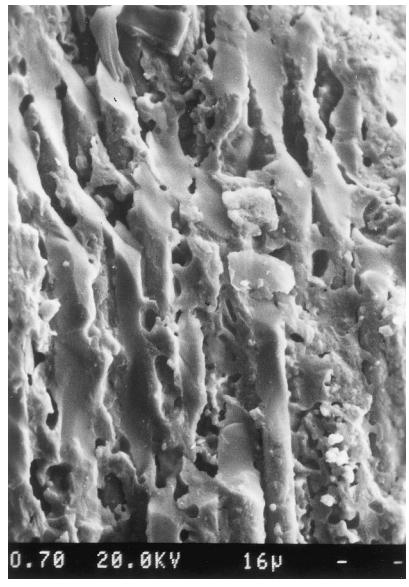

Fig. 11. SEM micrograph of the fracture surface of [90°] composite specimen being crept for 21·5 h at $T = 1150$°C and 40 MPa.

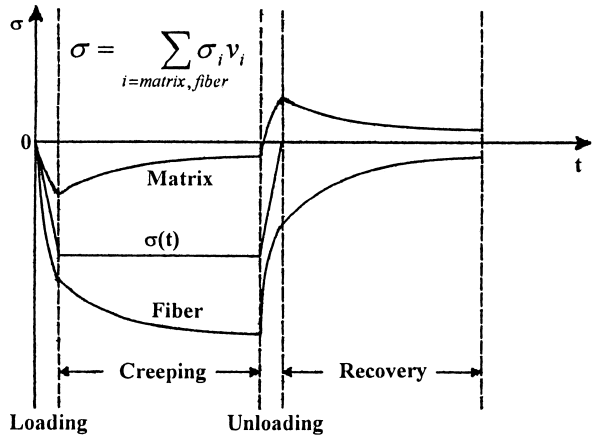

Fig. 12. Schematic representation of the axial stress redistribution between the SiC fibers and the mullite matrix for the [0°] composite during compressive creep and creep recovery.

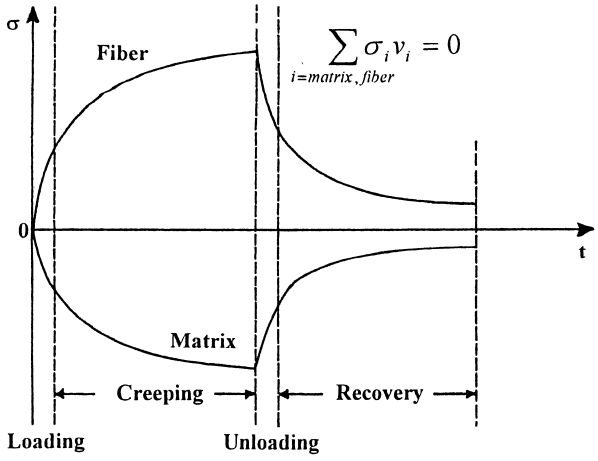

Fig. 13. Schematic representation of the stress redistribution between the SiC fibers and the mullite matrix for the [90°] composite during compressive creep and creep recovery, where the stress is parallel to the fiber direction.

the SiC fibers is much higher than that of the mullite matrix for our composites, the stress on mullite matrix would be transferred gradually to the SiC fibers during transient creep for the [0°] composite. The SiC fibers in the [0°] composite would suffer most part of the applied stress during creeping. After removing the load, there is a residual stress state between the SiC fibers and mullite matrix in the [0°] composite (Fig. 12), which is similar to the situation of fiber-reinforced composites creep tested in tension.[13,14] The relaxation of this residual stress state on load removal would result in the strain-recovery behavior of the [0°] composite (Fig. 7).

For the [90°] composite, there is a couple of stresses between the SiC fibers and the mullite matrix during creep tests (Fig. 13), due to the friction between the SiC fibers and the mullite matrix under the compressive stress, where the stress is parallel to the fiber direction. The SiC fibers are in tension and the mullite matrix is in compression. The sum of the stress on the fibers and matrix is zero. During transient creep stage, this couple of stresses increases gradually, until a stable creep stage reaches. After removing the load, the stress on the fibers and the matrix would be relaxed (Fig. 13). The relaxation of the residual stress state between the SiC fibers and the mullite matrix on load removal would cause an apparent creep-recovery behavior in the [90°] composite (Fig. 8).

The creep-recovery behavior verifies the different creep-resistance improvement mechanisms in the two composites, and *vice versa*. The improvement in creep resistance of the [0°] composite is realized by shedding most part of the applied stress on the

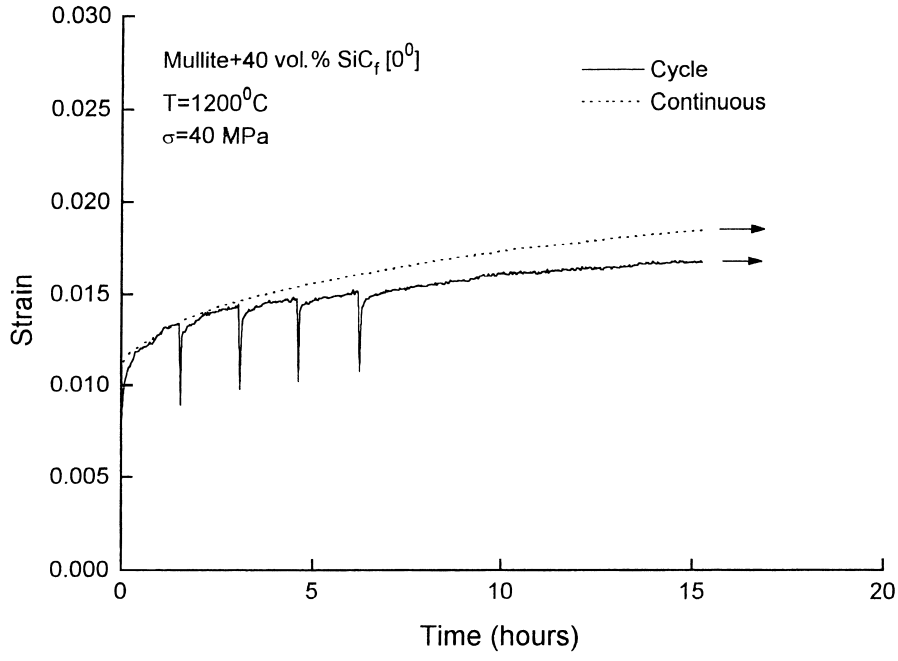

Fig. 14. Comparison of the creep behavior of the [0°] composite under constant loading with that under cyclically loading, where the recovery parts of the creep curve under cyclically loading were deleted.

SiC fibers, and the improvement in creep resistance of the [90°] composite is produced by the SiC fibers inhibiting the sliding of matrix mullite grains along the fibers. Because the reinforcement of SiC fibers is more effective for the [0°] composite compared to the [90°] composite, the improvement in the creep resistance for the [0°] composite is more apparent than that for the [90°] composite. In addition, when the loading-unloading cycle increases, the total creep strain increases, the duration of the transient creep in a cycle decreases, and the creep strain in the cycle decreases (Figs 7 and 8). Two reasons can explain that the total-strain recovery ratio R_t decreases and the creep-strain recovery ratio R_{cr} increases with the increase in the creep cycle. Strain-recovery behavior provides a convincing mechanism for the reduction of creep strain during cyclic creep (Fig. 14), where the creep strain of the [0°] composite under cyclically loading is apparently smaller than that under constant loading for the same loading time. In the absence of cyclic crack growth, the strain-recovery is expected to significantly increase the life of cyclically loaded structures.

5 Conclusions

The compressive creep behavior of monolithic mullite and two types of composites with different fiber orientations were investigated: one with the SiC fibers parallel to the loading direction ([0°] composite), and the other with the SiC fibers, perpendicular to the loading direction ([90°] composite). The following results were obtained.

1. The glass-containing mullite matrix showed considerable deformation due to the viscous flow of the glassy phase. However, the two types of composites with SiC fibers both exhibited excellent creep resistance compared with the creep behavior of monolithic mullite. The creep strain rate of the [0°] composite is about three orders of magnitude lower than that of monolithic mullite, and the creep strain rate of the [90°] composite is only 4–6 times higher than that of the [0°] composite.
2. A model based on the rule of mixtures was used. It showed that, the creep behavior of the [0°] composite is governed by the creep property of the SiC fibers, while the creep behavior of the [90°] composite is governed by the creep property of the mullite matrix.
3. The difference between the model and experimental results for the [90°] composite is believed to be due to the friction between the SiC fibers and the mullite matrix during creeping. This friction effect inhibits the sliding of matrix mullite grains along the fiber surfaces and results in the considerable improvement in the creep resistance of the [90°] composites as compared with the monolithic material.
4. There is an apparent creep-recovery behavior for the two types of composites, due to the relaxation of the residual stress state between the SiC fibers and the mullite matrix on load-removal. In addition, strain-recovery behavior reduces the total creep strain during cyclic creep, compared with the creep strain under constant load.

Acknowledgements

This work was supported by NEDO in Japan and National Natural Science Foundation of China.

References

1. Singh, R. N. and Gaddipati, A. R., Mechanical properties of a uniaxially reinforced mullite-silicon carbide composite. *J. Am. Ceram. Soc.*, 1988, **71**(2), C100–C103.
2. Kodama, H., Sakamoto, H. and Miyoshi, T., Silicon carbide monofilament-reinforced silicon nitride or silicon carbide matrix composites. *J. Am. Ceram. Soc.*, 1989, **72**(4), 551–558.
3. Kerans, R. J., Parthasarathy, T. A., Jero, P. D., Chatterjee, A. and Pagano, N. J., Fracture and sliding in the fibre/matrix interface and failure processes in ceramic composites. *Br. Ceram. Trans.*, 1993, **92**(5), 181–196.
4. Singh, D., Singh, J. P., Majumdar, S., Kupperman, D. S., Cowdin, E. and Bhatt, R. T., Effect of processing variables on interfacial properties of an SiC-fiber-reinforced reaction-bonded Si_3N_4 matrix composite. *J. Am. Ceram. Soc.*, 1994, **77**(10), 2561–2568.
5. Abbe, F., Vicens, J. and Chermant, J. L., Creep behaviour and microstructural characterization of a ceramic matrix composite. *J. Mater. Sci. Lett.*, 1989, **8**, 1026–1028.
6. Abbe, F., Chermant, L., Coster, M., Gomina, M. and Chermant, J. L., *Comp. Sci. Tech*, 1990, **37**, 109–127.
7. Chermant, J. L., *Sil Ind.*, 1995, **60**, 261–273.
8. Vicens, J., Doreau, F. and Chermant, J. L., *J. Microscopy*, 1997, **185**, 168–177.
9. Boitier, G., Vicens, J. and Chermant, J. L., Tensile creep results on a C_f-SiC composite. *Script. Mater.*, 1997, **37**(12), 1923–1929.
10. Evans, A. G. and Weber, C., Creep damage in SiC/SiC composites. *Mater. Sci. Eng.*, 1996, **A208**, 1–6.
11. Zhu, S. J., Mizuno, M., Kagawa, Y., Cao, J. W., Nagano, Y. and Kaya, H., Creep and fatigue behavior of SiC fiber reinforced SiC composite at high temperatures. *Mater. Sci. Eng.*, 1997, **A225**, 69–77.
12. Zhu, S. L., Mizuno, M., Nagano, Y., Cao, J. W., Kagawa, Y. and Kaya, H., Creep and fatigue behavior in an enhanced SiC/SiC composite at high temperatures. *J. Am. Ceram. Soc.*, 1998, **81**(9), 2269–2277.
13. Holmes, J. W., Park, Y. H. and Jones, J. W., Tensile creep and creep-recovery behavior of a SiC-fiber–Si_3N_4-matrix composite. *J. Am. Ceram. Soc.*, 1993, **76**(5), 1281–1293.
14. Wu, X. and Holmes, J. W., Tensile creep and creep-strain recovery behavior of silicon carbide fiber/calcium aluminosilicate matrix ceramic composites. *J. Am. Ceram. Soc.*, 1993, **76**(10), 2695–2700.
15. Weber, C. H., Löfvander, J. P. A. and Evans, A. G., Creep anisotropy of a continuous-fiber-reinforced silicon

carbide/calcium aluminosilicate composite. *J. Am. Ceram. Soc.*, 1994, **77**(7), 1745–1752.
16. Thayer, R. B. and Yang, J. M., Analysis of flexural creep for an SiC fiber-reinforced Si_3N_4 composite. *J. Mater. Sci.*, 1994, **29**, 693–699.
17. Prochazka, S. and Klug, F. J., Infrared-transparent mullite ceramic. *J. Am. Ceram. Soc.*, 1983, **66**(12), 874–880.
18. Osendi, M. I. and Baudin, C., Mechanical properties of mullite materials. *J. Eur. Ceram. Soc.*, 1995, **16**, 217–224.
19. Mah, T., Hecht, N. L., McCullum, D. E., Hoenigman, J. R., Kim, H. M., Katz, A. P. and Lipsitt, H. A., Thermal stability of SiC fibers (Nicalon®). *J. Mater. Sci.*, 1984, **19**, 1191–1201.
20. Yamada, Y., Kawaguchi, Y., Takeda, N. and Kishi, T., Interfacial debonding behavior of mullite/SiC continuous fiber composite. *J. Am. Ceram. Soc.*, 1995, **78**(12), 3209–3216.
21. Ohira, H., Ismail, M. G. M. U., Yamamoto, Y., Akiba, T. and Somiya, S., Mechanical properties of high purity mullite at elevated temperatures. *J. Am. Ceram. Soc.*, 1996, **16**, 225–229.
22. Deng, Z. Y., Ph.D. Thesis, Shanghai Institute of Ceramics, 1996.
23. Cannon, W. R. and Langdon, T. G., Review creep of ceramics, Part 1 Mechanical characteristics. *J. Mater. Sci.*, 1983, **18**, 1–50.
24. Hynes, A. P. and Doremus, R. H., High-temperature compressive creep of polycrystalline mullite. *J. Am. Ceram. Soc.*, 1991, **74**(10), 2469–2475.
25. Gu, W. Z., Porter, J. R. and Langdon, T. G., Evidence for anelastic creep recovery in silicon carbide-whisker-reinforced alumina. *J. Am. Ceram. Soc.*, 1994, **77**(6), 1679–1681.
26. Okamoto, Y., Fukudome, H., Hayashi, K. and Nishikawa, T., Creep deformation of polycrystalline mullite. *J. Eur. Ceram. Soc.*, 1990, **6**, 161–168.
27. Ohira, H., Shiga, H., Ismail, M. G. M. U., Nakai, Z., Akiba, T. and Yasuda, E., Compressive creep of mullite ceramics. *J. Mater. Sci. Lett.*, 1991, **10**, 847–849.
28. Zhang, Y. F., Guo, J. K., Yang, H. M., Zhu, P. N. and Huang, S. Z., SiC fiber-reinforced lithium aluminosilicate matrix composites. *Mater. Sci. Progress*, 1992, **6**(3), 265–267 (in Chinese).
29. Bodet, R., Bourrat, X., Lamon, J. and Naslain, R., Tensile creep behavior of a silicon carbide-based fiber with a low oxygen content. *J. Mater. Sci.*, 1995, **30**, 661–677.
30. De Silva, A. R. T., A theoretical analysis of creep in fibre reinforced composites. *J. Mech. Phys. Solids*, 1968, **16**, 169–186.
31. Simon, G. and Bunsell, A. R., Creep behavior and structural characterization at high temperatures of Nicalon SiC fibers. *J. Mater. Sci.*, 1984, **19**, 3658–3670.